J|A|C|S
ARTICLES
Published on Web 05/28/2006

Direct Observation of Salt Effects on Molecular Interactions through Explicit-Solvent Molecular Dynamics Simulations: Differential Effects on Electrostatic and Hydrophobic Interactions and Comparisons to Poisson−Boltzmann Theory

Andrew S. Thomas and Adrian H. Elcock*

Contribution from the Department of Biochemistry, University of Iowa, Iowa City, Iowa 52242

Received December 20, 2005; E-mail: adrian-elcock@uiowa.edu

Abstract: Proteins and other biomolecules function in cellular environments that contain significant concentrations of dissolved salts and even simple salts such as NaCl can significantly affect both the kinetics and thermodynamics of macromolecular interactions. As one approach to directly observing the effects of salt on molecular associations, explicit-solvent molecular dynamics (MD) simulations have been used here to model the association of pairs of the amino acid analogues acetate and methylammonium in aqueous NaCl solutions of concentrations 0, 0.1, 0.3, 0.5, 1, and 2 M. By performing simulations of 500 ns duration for each salt concentration properly converged estimates of the free energy of interaction of the two molecules have been obtained for all intermolecular separation distances and geometries. The resulting free energy surfaces are shown to give significant new insights into the way salt modulates interactions between molecules containing both charged and hydrophobic groups and are shown to provide valuable new benchmarks for testing the description of salt effects provided by the simpler but faster Poisson−Boltzmann method. In addition, the complex many-dimensional free energy surfaces are shown to be decomposable into a number of one-dimensional effective energy functions. This decomposition (a) allows an unambiguous view of the qualitative differences between the salt dependence of electrostatic and hydrophobic interactions, (b) gives a clear rationalization for why salt exerts different effects on protein−protein association and dissociation rates, and (c) produces simplified energy functions that can be readily used in much faster Brownian dynamics simulations.

Introduction

Most biological molecules, whether in living cells or on the lab bench, are immersed in aqueous salt solutions and it has long been appreciated that salts can exert significant, and sometimes profound effects on the behavior of biomolecules. Well-known examples include the widely varying influences of salts on protein solubility exemplified by the Hofmeister effect,[1,2] the effects of salt on DNA duplex stability,[3] and on the thermodynamics and kinetics of electrostatically driven protein-DNA[4,5] and protein−protein associations.[6−8] Since significant salt concentrations are routinely encountered by biological macromolecules in physiological conditions, a thorough understanding of the ways salts affect thermodynamic and kinetic properties may ultimately be important for understanding their in vivo behavior. The present work therefore describes the use of explicit solvent molecular dynamics (MD) simulations aimed specifically at understanding the effects of the simple salt NaCl on a prototypical biomolecular association event in which both hydrophobic and electrostatic interactions operate between the solutes.

As might be expected, MD simulations have been used extensively over the years to investigate many of the key effects of salt on aqueous solutions. Most such studies have however not considered biomolecular association events but instead have focused on the behavior of solute-free salt solutions. A number of different aspects have been examined including the effects of different ion types on water structure,[9,10] the connection between such effects and hydration thermodynamics,[11−16] and the tendencies for ions to form clusters.[17,18] In addition, studies focused solely on single-ion-in-water systems have also proven

(1) Baldwin, R. L. *Biophys. J.* **1996**, *71*, 2056−2063.
(2) Collins, K. D. *Methods* **2004**, *34*, 300−311.
(3) Manning, G. S. *Biophys. Chem.* **2002**, *101*, 461−473.
(4) Misra, V. K.; Hecht, J. L.; Sharp, K. A.; Friedman, R. A.; Honig, B. *J. Mol. Biol.* **1994**, *238*, 264−280.
(5) Zhang, W.; Bond, J. P.; Anderson, C. F.; Lohman, T. M.; Record, M. T. *Proc. Natl. Acad. Sci. U.S.A.* **1996**, *93*, 2511−2516.
(6) Mei, H.; Wang, K.; McKey, S.; Wang, X.; Waldner, J. L.; Pielak, G. J.; Durham, B.; Millett, F. *Biochemistry* **1996**, *35*, 15800−15806.
(7) Radic, Z.; Kirchhoff, P. D.; Quinn, D. M.; McCammon, J. A.; Taylor, P. *J. Biol. Chem.* **1997**, *272*, 23265−23277.
(8) Selzer, T.; Schreiber, G. *J. Mol. Biol.* **1999**, *287*, 409−419.
(9) Chowdhuri, S.; Chandra, A. *J. Chem. Phys.* **2001**, *115*, 3732−3741.
(10) Hribar, B.; Southall, N. T.; Vlachy, V.; Dill, K. A. *J. Am. Chem. Soc.* **2002**, *124*, 12302−12311.
(11) Smith, D. E.; Haymet, A. D. J. *J. Chem. Phys.* **1993**, *98*, 6445−6454.
(12) Chitra, R.; Smith, P. E. *J. Phys. Chem. B* **2002**, *106*, 1491−1500.
(13) Asthagiri, D.; Pratt, L. R.; Ashbaugh, H. S. *J. Chem. Phys.* **2003**, *119*, 2702−2708.
(14) Grossfield, A.; Ren, P.; Ponder, J. W. *J. Am. Chem. Soc.* **2003**, *125*, 15671−15682.
(15) Rajamani, S.; Ghosh, T.; Garde, S. *J. Chem. Phys.* **2004**, *120*, 4457−4466.
(16) Grossfield, A. *J. Chem. Phys.* **2005**, *122*, 024506.
(17) Degrève, L.; da Silva, F. L. B. *J. Chem. Phys.* **1999**, *111*, 5150−5156.
(18) Zahn, D. *Phys. Rev. Lett.* **2004**, *92*, 040801.

10.1021/ja058637b CCC: $33.50

to be extremely useful for developing an understanding of how to deal with long-range electrostatic interactions adequately in molecular simulations.[19,20]

Most of the MD studies that have directly addressed the effects of salts on molecular associations have focused primarily on the association of simple hydrophobic molecules (such as methane) whose association is thought to be significantly strengthened by salts at high concentrations (~1 M). Some of these studies have limited their attention to the effects of high salt concentrations on the *hydration* of hydrophobic molecules,[21,22] but others have explicitly examined the effects of salt on *associations* through computation of potentials of mean force as a function of intermolecular distance between two hydrophobic solutes.[23,24]

Perhaps surprisingly, MD simulations of the effects of salt on electrostatically driven biomolecular association events are harder to find; in fact, to our knowledge the only example is a very recent study of salt effects on amino acids using relatively short (15 ns) constrained potential of mean force (PMF) calculations.[25] Instead, the understanding of salt effects on electrostatic interactions has relied more on traditional theoretical treatments such as counterion condensation theory[26,27] and the Poisson−Boltzmann equation.[28] Since the latter method can be routinely used to study atomically detailed structures of arbitrary geometry it has become the method of choice for most biomolecular applications;[29] numerical solutions of the PB equation have even been reported for molecular assemblies as large as the ribosome.[30] Atomically detailed PB calculations have been successfully used to understand the effects of monovalent ions on the thermodynamics of ligand−DNA interactions,[31] protein−DNA interactions[4,32] and protein stability.[33,34] In addition, the electrostatic potentials obtained from PB theory have been used in Brownian dynamics (BD) simulations to understand the effects of salt on the kinetics of protein−protein association events;[35−37] interestingly, these effects have also been successfully modeled with simple Debye−Hückel calculations.[38,39] Relative to explicit-solvent MD simulations, PB theory makes two major simplifications: the solvent is treated as a dielectric continuum and the distribution of dissolved ions is treated as continuous and adequately modeled with a mean-field treatment that neglects ion−ion correlations. The validity of the first of these simplifications has been examined in a number of studies by comparison of hydration and binding thermodynamics obtained from PB with those obtained from explicit-solvent MD simulations.[40−43] Although these comparisons have highlighted some anticipated failings of PB, the level of agreement is in general sufficiently good that it is now often used as a "gold standard" for testing of still more approximate implicit solvent methods.[44,45]

One motivation of the present work is to show that both major simplifications of PB theory—i.e., its description of water *and* ions—can now be simultaneously tested through the use of MD methods of the kind now widely used to simulate the dynamic behavior of biological macromolecules.[46] In principle, it should be clear that MD simulations can provide a much more structurally detailed and thermodynamically refined view of salt effects than can be obtained by PB theory. In practice, however, this can only be done if sufficient sampling of the ion, water and solute configurations can be performed with MD to obtain converged thermodynamic information, and one goal of the present work is to examine whether current computational resources allow this to be achieved. In examining this issue, we aim to build on recent work performed by ourselves and others showing that the association thermodynamics (equilibrium constants) for small molecule pairs in water can be directly computed from unforced explicit solvent MD simulations in which the interacting molecules are left to freely diffuse throughout the solution and associate with one another by any pathway that they might choose.[47−49] These previous studies considered a range of molecule types from complete amino acids to smaller prototypical molecules, but—importantly for the present study—were all performed in pure water. There is clearly an additional level of sampling required when the solvent, as in the case of an aqueous salt solution, is of a heterogeneous composition and it is therefore a key result of the present work that the same basic approach used previously—but with MD simulations that are 500 ns in length—can be used to obtain converged results for small molecule associations in salt solutions.

We have chosen to study the effects of NaCl on the association of the small molecules acetate and methylammonium. These molecules have been selected for two reasons. First, they can be considered to be simplified analogues of the charged amino acid side chains glutamate/aspartate and lysine, for which salt effects are likely to be considerable; the decision to use simpler, prototypical molecules rather than actual amino side chains has been based on our previous experience of the difficulties in disentangling the various driving forces that operate even in molecules as apparently simple as amino acids.

(19) Hummer, G.; Pratt, L. R.; Garcia, A. E. *J. Phys. Chem. A* **1998**, *102*, 7885−7895.
(20) Bergdorf, M.; Peter, C.; Hünenberger, P. H. *J. Chem. Phys.* **2003**, *119*, 9129−9144.
(21) Smith, P. E. *J. Phys. Chem. B* **1999**, *103*, 525−534.
(22) van der Vegt, N. F. A.; van Gunsteren, W. F. *J. Phys. Chem. B* **2004**, *108*, 1056−1064.
(23) Ghosh, T.; Garcia, A. E.; Garde, S. *J. Phys. Chem. B* **2003**, *107*, 612−617.
(24) Ghosh, T.; Kalra, A.; Garde, S. *J. Phys. Chem. B* **2005**, *109*, 642−651.
(25) Hassan, S. A. *J. Phys. Chem. B* **2005**, *109*, 21989−21996.
(26) Manning, G. S. *J. Chem. Phys.* **1969**, *51*, 924−933.
(27) Record, M. T.; Lohman, T. M.; de Haseth, P. *J. Mol. Biol.* **1976**, *107*, 145−158.
(28) Honig, B.; Nicholls, A. *Science* **1995**, *268*, 1144−1149.
(29) Fogolari, F.; Brigo, A.; Molinari, H. *J. Mol. Recognit.* **2002**, *15*, 377−392.
(30) Baker, N. A.; Sept, D.; Joseph, S.; Holst, M. J.; McCammon, J. A. *Proc. Natl. Acad. Sci. U.S.A.* **2001**, *98*, 10037−10041.
(31) Misra, V. K.; Sharp, K. A.; Friedman, R. A.; Honig, B. *J. Mol. Biol.* **1994**, *238*, 245−263.
(32) Zacharias, M.; Luty, B. A.; Davis, M. E.; McCammon, J. A. *Biophys. J.* **1992**, *63*, 1280−1285.
(33) Elcock, A. H.; McCammon, J. A. *J. Mol. Biol.* **1998**, *280*, 731−748.
(34) Dominy, B. N.; Perl, D.; Schmid, F. X.; Brooks, C. L. *J. Mol. Biol.* **2002**, *319*, 541−554.
(35) Gabdoulline, R. R.; Wade, R. C. *Biophys. J.* **1997**, *72*, 1917−1929.
(36) Elcock, A. H.; Gabdoulline, R. R.; Wade, R. C.; McCammon, J. A. *J. Mol. Biol.* **1999**, *291*, 149−162.
(37) Gabdoulline, R. R.; Wade, R. C. *J. Mol. Biol.* **2001**, *306*, 1139−1155.
(38) Selzer, T.; Albeck, S.; Schreiber, G. *Nat. Struct. Biol.* **2000**, *7*, 537−541.
(39) Zhou, H.-X. *Biopolymers* **2001**, *59*, 427−433.
(40) Jean-Charles, A.; Nicholls, A.; Sharp, K.; Honig, B.; Tempczyk, A.; Hendrickson, T. F.; Still, W. C. *J. Am. Chem. Soc.* **1991**, *113*, 1454−1455.
(41) Zhang, L. Y.; Gallicchio, E.; Friesner, R. A.; Levy, R. M. *J. Comput. Chem.* **2001**, *22*, 591−607.
(42) Wagoner, J.; Baker, N. A. *J. Comput. Chem.* **2004**, *25*, 1623−1629.
(43) Yu, Z.; Jacobson, M. P.; Josovitz, J.; Rapp, C. S.; Friesner, R. A. *J. Phys. Chem. B* **2004**, *108*, 6643−6654.
(44) Feig, M.; Onufriev, A.; Lee, M. S.; Im, W.; Case, D. A.; Brooks, C. L *J. Comput. Chem.* **2004**, *25*, 265−284.
(45) Feig, M.; Brooks, C. L. *Curr. Opin. Struct. Biol.* **2004**, *14*, 217−224.
(46) Karplus, M.; McCammon, J. A. *Nat. Struct. Biol.* **2002**, *9*, 646−652.
(47) Zhang, Y.; McCammon, J. A. *J. Chem. Phys.* **2003**, *118*, 1821−1827.
(48) Yang, H. B.; Elcock, A. H. *J. Am. Chem. Soc.* **2003**, *125*, 13968−13969.
(49) Thomas, A. S.; Elcock, A. H. *J. Am. Chem. Soc.* **2004**, *126*, 2208−2214.

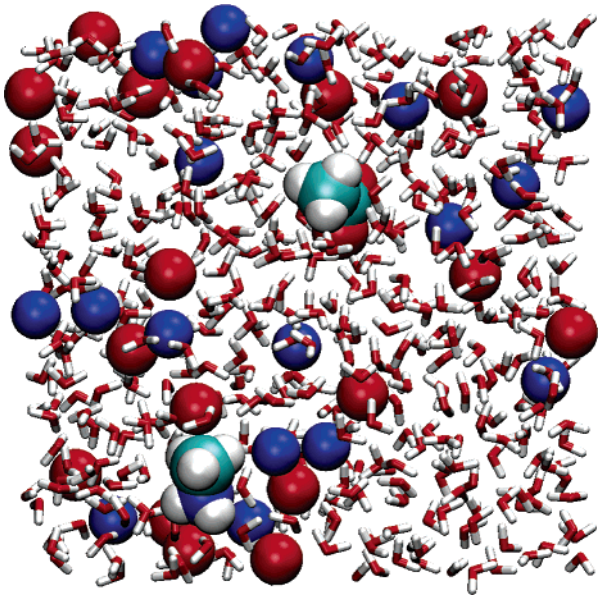

Figure 1. Illustration of the acetate−methylammonium pair in a 2 M NaCl solution. Acetate and methylammonium are shown in space-filling representations; water molecules are shown as licorice bonds; Na^+ and Cl^- ions are shown as blue and red spheres, respectively.

Second, the two molecules contain both charged *and* hydrophobic groups, and it is therefore possible for them to associate with one another via an electrostatic (salt bridge) interaction, via a hydrophobic interaction (through juxtaposition of their methyl groups), or perhaps via some combination of the two (e.g., in a side-by-side orientation). The simulated association behavior of these two very simple molecules therefore has the potential to provide quite rich information into the interplay and balance between charge−charge and hydrophobic interactions and the differential effects of salt on these different types of interaction. As becomes apparent, however, to fully understand these different effects, it proves necessary to develop a scheme for decomposing the many-dimensional free energy surface obtained from the simulations into one-dimensional effective energy functions that can be more easily interpreted. This decomposition has the added benefit however of yielding simple pairwise energy functions that may in the future be useful for simulation methods (such as BD) in which salt ions and water molecules are modeled implicitly.

Methods

MD Simulations. Each of the six 500 ns MD simulations discussed here contained a single acetate and a single methylammonium molecule immersed in a 25 × 25 × 25Å box of explicit solvent. One simulation was performed in pure water and five others were performed at the following NaCl concentrations: 0.1, 0.3, 0.5, 1, and 2 M; the number of Na^+ and Cl^- ions included in these simulations was 1, 3, 5, 9, and 18, respectively. An illustration of the 2 M NaCl simulation system is shown in Figure 1. Parameters for the acetate and methylammonium were obtained from the OPLS-AA force field[50] with the partial charges being adapted from those assigned in the force field to glutamate and lysine respectively (see Table 1 of Supporting Information). Parameters for the Na^+ and Cl^- ions were obtained from works by Aqvist[51] and Jorgensen and co-workers;[52] water molecules were described by the TIP3P model.[53] Although there may be significant polarization effects involved in highly charged systems such as aqueous ionic solutions, previous simulation work has indicated that nonpolarizable force fields remain surprisingly useful for modeling such systems.[16,54]

All MD simulations were performed with the GROMACS software.[55,56] van der Waals and short-range electrostatic interactions were truncated at 10Å; longer range electrostatic interactions were calculated using the PME method.[57] All covalent bonds were constrained with the LINCS algorithm[58] allowing a 2 fs time step to be used. Simulations were performed in the NPT ensemble (constant number of atoms, pressure and temperature) with the pressure being maintained at 1atm using the Parrinello−Rahman barostat[59] and the temperature being maintained at 298 K using the Nosé−Hoover thermostat.[60,61] Since the strong interaction between salt ions and water molecules causes a modest contraction of the periodic box (since the box volume is not constrained), short pilot simulations were conducted to ensure that the final molar concentrations of salt were close to their intended values. All simulation systems were initially energy minimized for 100 steps with the steepest-descent algorithm, heated in 50K steps at intervals of 50 ps and equilibrated for 10 ns; following this point each system was simulated for an additional 500 ns. An indication that this length of simulation is likely to be sufficient for properly sampling both the associated and dissociated states is that in the case of the pure water simulation a total of 525 independent association events were observed (with each separate event being considered to begin when the charged groups reached a separation of 10Å, and to end when both the charged and hydrophobic groups came within 0.2Å of their separations in the global minimum configuration; see Results). During simulations, atomic coordinates were saved every 0.1 ps, thereby yielding five million structural snapshots per simulation system for further data analysis.

Free Energy Surface Calculations. Free energy surfaces for the interaction of acetate and methylammonium were computed by constructing histograms of inter-solute atomic distances extracted from the simulation snapshots. At first sight, it might be thought that separate free energy profiles for the charge−charge and hydrophobic interactions could be directly obtained simply by constructing and analyzing separate histograms for the two dimensions (e.g., a one-dimensional histogram of charge−charge distances could be used to compute a free energy profile for the charge−charge interaction). However, as has been recognized by others in somewhat different contexts,[62] when different types of interacting groups are located near or adjacent to one another in a molecule their effective interactions can be so tightly coupled that they cannot really be considered to be independent of one another. This makes examining the charge−charge and hydrophobic interactions by constructing separate one-dimensional histograms potentially very misleading.

The simplest way around this problem, and as it turns out also the most visually informative way of describing the interaction, was found to be to construct two-dimensional histograms and free energy surfaces (2D-FESs) in which one dimension is the distance between the two charged groups of the molecules (specifically the $C_{carboxyl}$ to N_{amino} distance) and the second dimension is the distance between the two hydrophobic groups (the C_{methyl} to C_{methyl} distance). For a more complete analysis of the interaction thermodynamics—albeit one that does not

(50) Kaminski, G. A.; Friesner, R. A.; Tirado-Rives, J.; Jorgensen, W. L. *J. Phys. Chem. B* **2001**, *105*, 6474−6487.
(51) Aqvist, J. *J. Phys. Chem.* **1990**, *94*, 8021−8024.
(52) Chandrasekhar, J.; Spellmeyer, D. C.; Jorgensen, W. L. *J. Am. Chem. Soc.* **1984**, *106*, 903−910.
(53) Jorgensen, W. L.; Chandrasekhar, J.; Madura, J. D.; Impey, R. W.; Klein, M. L. *J. Chem. Phys.* **1983**, *79*, 926−935.
(54) Smith, D. E.; Dang, L. X. *J. Chem. Phys.* **1994**, *100*, 3757−3766.
(55) Lindahl, E.; Hess, B.; van der Spoel, D. *J. Mol. Mod.* **2001**, *7*, 306−317.
(56) Berendsen, H. J. C.; van der Spoel, D.; van Drunen, R. *Comput. Phys. Comm.* **1995**, *91*, 43−56.
(57) Essman, U.; Perela, L.; Berkowitz, M. L.; Darden, T.; Lee, H.; Pedersen, L. G. *J. Chem. Phys.* **1995**, *103*, 8577−8592.
(58) Hess, B.; Bekker, H.; Berendsen, H. J. C.; Fraaije, J. G. E. M. *J. Comput. Chem.* **1997**, *18*, 1463−1472.
(59) Parrinello, M.; Rahman, A. *J. Appl. Phys.* **1981**, *52*, 7182−7190.
(60) Nosé, S. J. *J. Chem. Phys.* **1984**, *81*, 511−519.
(61) Hoover, W. G. *Phys. Rev. A* **1985**, *31*, 1695−1697.
(62) Thomas, P. D.; Dill, K. A. *Proc. Natl. Acad. Sci. U.S.A.* **1996**, *93*, 11628−11633.

lend itself to visual inspection—four-dimensional free energy surfaces (4D-FESs) were also constructed in which the additional dimensions were the two $O_{carboxyl}$ to N_{amino} distances. To construct the 2-dimensional histograms bin widths of 0.1Å were used for both distances; to construct the 4-dimensional histograms coarser bin widths of 0.2Å were used because of the sparser sampling in 4D space.

It is important to note that in histograms constructed in this way the population within each distance bin will be determined not only by the effective strength of the interaction between the two solutes at that distance, but also by the number of ways that the two solutes can be arranged within the simulation box with that distance. Since it is the former that we are interested in, we must first subtract out the latter contribution—which in effect represents a configurational entropy term—in order to obtain an effective interaction free energy surface. We do this by comparing the MD-simulated histograms with reference histograms that are constructed from additional simulations in which the two solutes do not physically interact with one another. In previous work we have constructed these reference histograms simply by performing repeated random placements of the two solutes—modeled fixed in their equilibrium conformations—into the periodic simulation box. In the current work the reference histograms have instead been obtained by running very long (7.5 μs) stochastic dynamics (SD) simulations of the two solutes with all intermolecular interactions turned off while retaining the intramolecular parameters of the "true" MD simulations. This latter approach has the advantage that it ensures that the (minor) fluctuations that naturally occur in the internal geometries of the solutes are present in both the MD-simulated and reference histograms and do not therefore serve as a unnecessary source of noise.

Having converted the 2D MD-simulated and reference histograms into probability distributions, the (excess) interaction free energies can be calculated using:

$$\Delta G^\circ(i,j) = -RT \ln [P_{\text{interacting}}(i,j)/P_{\text{non-interacting}}(i,j)]$$

where $\Delta G^\circ(i,j)$ is the interaction free energy of the i,jth bin on the 2D-FES, $P_{\text{interacting}}$ and $P_{\text{non-interacting}}$ are the probabilities of occupancy of that bin obtained from the MD-simulated and reference histograms respectively, R is the Gas Constant, and T is the temperature. An analogous equation, though of course with additional dimensions, is used to compute the 4D-FES.

The procedure outlined above only allows *relative* interaction free energy surfaces to be computed: for example, the difference in interaction free energies of two bins on the same 2D-FES can be obtained simply by subtracting the $\Delta G^\circ(i,j)$ values computed for the two bins. What it does not do is enable us to place these free energy surfaces on an *absolute* scale; to do this we must be able to match at least some of the computed values with known $\Delta G^\circ(i,j)$ values. For systems with no long-range electrostatic interactions, it would be possible to simply assume that the computed $\Delta G^\circ(i,j)$ values must become zero at long intermolecular distances, and find the additive constant that best enforces this behavior. But in the present case, there are significant interactions between the two solutes even at comparatively long distances (e.g., 12 Å) and the simulation box is not large enough that we can reach a distance where the interaction can truly be assumed to be zero. To circumvent this problem we instead assume that at long distances the interaction between the two solutes can be accurately described by Poisson−Boltzmann theory; as will be shown below the results justify this assumption. We therefore find the additive constant necessary to convert the relative 2D-FES into an absolute 2D-FES by linear regression of the former with a corresponding 2D-FES calculated with Poisson−Boltzmann (PB) theory (details outlined below). Because there is reason to expect that MD- and PB-computed free energies may be in poor agreement at short intermolecular distances, this regression was performed using only those 2D bins in which both the inter-charge and inter-methyl distances were between 10 and 15Å (see Figure S1), these bins being chosen because they are the most highly sampled during the reference SD simulations.

Poisson−Boltzmann Calculations. All Poisson−Boltzmann calculations were performed with the electrostatics program UHBD.[63] PB 2D-FESs corresponding to the MD 2D-FESs were computed as follows. The 5 million structural snapshots sampled during each MD simulation were assigned to the appropriate 2D histogram bins, and five snapshots from each bin were randomly selected. The direct electrostatic interaction energy between the two solutes was calculated by solving the PB equation for all five of these snapshots and the average of the five energies was used to construct the 2D-FES. In practice, there was very little difference between the five computed interaction energies at long distances: the standard deviation was around 3−5% at ∼12Å separation; however, as might be expected, at much shorter distances standard deviations of ∼20−50% were obtained. In all PB calculations, the partial charges assigned to atoms were identical to those used in the MD simulations; atomic radii were taken from the PARSE parameter set.[64] All calculations used a solvent dielectric of 78.4 and a solute dielectric of 12. Additional calculations were also performed using a solute dielectric of 2 and (separately) a solvent dielectric of 92 (corresponding to the dielectric of TIP3P water)[65] but produced results that did not differ significantly (data not shown). The boundary between solute and solvent dielectric regions was defined by the molecular surface as calculated with a solvent probe radius of 1.4 Å. In contrast to the way that PB calculations are usually conducted, regions of space that were assigned the solvent dielectric value were also considered to be accessible to dissolved ions, i.e., no ion-exclusion radius (Stern layer) was applied. This decision was based on the finding that calculations conducted with the more usual ion-exclusion radius of 2 Å produced results that were in poorer agreement with the MD results (see Results; Supporting Information). All PB calculations were performed in two stages using the technique of "focusing".[66] In a first stage, the PB equation was solved on a relatively coarse $50 \times 50 \times 50$ grid of spacing 1 Å with the electrostatic potential at the boundary of the grid being set by applying the Debye−Hückel equation to the solute partial charges. In a second stage, the PB equation was solved on a much finer $100 \times 100 \times 100$ grid of spacing 0.25 Å with the electrostatic potentials at the boundary of the grid being interpolated from values obtained in the first stage calculation.

A simple comparison of the 2D-FES computed from these direct PB electrostatic calculations and the 2D-FES obtained from the explicit solvent-explicit salt MD simulations is hampered by the fact that the latter use the PME method to compute long-range electrostatic interactions. This means that in addition to the direct electrostatic interactions computed between the two solutes in the central simulation box, there are also "indirect" electrostatic interactions between a solute and the periodic images of the other solute. In principle, this can significantly affect the apparent long-range behavior of the inter-solute interaction: when the charged solutes are separated by a long distance their indirect interactions with periodic images become similar in magnitude to their direct interaction. More importantly, these indirect interactions would be present implicitly in the FES computed from the MD simulations but would be absent from the direct PB electrostatic energy calculations described above. It is to be noted that perhaps the simplest way to avoid this problem would be to perform the PB calculations with periodic boundary conditions applied; unfortunately however software that performs these kinds of calculations does not appear to be generally available. An alternative approach is to find a way to remove the indirect effects of the neighboring image boxes from the MD-simulation FES so that a MD FES that describes *only* the direct inter-solute interaction is obtained.

(63) Davis, M. E.; Madura, J. D.; Luty, B. A.; McCammon, J. A. *Comput. Phys. Commun.* **1991**, *62*, 187−197.
(64) Sitkoff, D.; Sharp, K. A.; Honig, B. *J. Phys. Chem.* **1994**, *98*, 1978−1988.
(65) Van der Spoel, D.; Van Maaren, P. J. *J Chem. Theory Comput.* **2006**, *2*, 1−11.
(66) Gilson, M. K.; Sharp, K. A.; Honig, B. H. *J. Comput. Chem.* **1988**, *9*, 327−335.

To accomplish this, we assume that the long-range indirect electrostatic interactions present in the MD simulations can themselves be approximated using PB theory.[20,67] With this assumption in mind, we proceed as follows. For each bin on the 2D-FES, three simulation snapshots were randomly selected (note that this is fewer than the five snapshots used to compute the direct PB interaction owing to the increased computational expense of the calculations). Two complete shells of images were then constructed around each snapshot (so that there was a total of 125 copies of each molecule—see Figure S2), and PB calculations were then performed to calculate the electrostatic interaction energy between the two solutes in the central box and the 124 surrounding image boxes. These calculations were performed using three stage focusing: a $50 \times 50 \times 50$ grid of spacing 2.5 Å was used to obtain boundary potentials for a $50 \times 50 \times 50$ grid of spacing 1 Å which in turn was used to obtain boundary potentials for a final $100 \times 100 \times 100$ grid of spacing 0.25 Å. These indirect electrostatic interaction energies were calculated only for the 0 M and 0.1 M MD-generated 2D-FESs since these had significant indirect electrostatic interactions (maximum energy of ~0.15 kcal/mol); for higher salt concentrations, pilot calculations of the PB-computed indirect contributions showed them to be insignificant (<0.02 kcal/mol) and so no correction for the periodicity effects was required. Interestingly, and providing support for the methodology outlined above, subtraction of the indirect contributions for the 0 M and 0.1 M salt systems substantially improved the agreement between the MD 2D-FES and the PB 2D-FES: for example, in the case of the 0 M system, the r^2 value for the regression of the two sets of data before correction for the indirect contribution was 0.74, whereas after correction it was 0.81 (see Figure S1 in Supporting Information).

Ion Distributions from MD and PB. To examine how Na^+ and Cl^- ions interact with the acetate and methylammonium solutes in the MD simulations, and to compare the observed behavior with the predictions of PB theory, local ion concentrations were obtained for a number of structures of interest in the 2D-FES. These comparisons were performed using structural snapshots taken from the 0.3 M NaCl MD simulation since this (a) contained a sufficient number of ions that adequate sampling of their configurations was readily obtained while (b) still being at a low enough salt concentration that PB theory should still be valid. The ion distributions from MD were obtained by superimposing all snapshot structures (solutes and ions) contained within the corresponding bins on the 2D histograms onto a single solute structure selected as representative of the geometry of interest. In practice, the representative solute structure chosen was the one having the lowest average RMSD from all other structures in the same sample. The ion distributions predicted by PB theory were obtained by solving the PB equation (on a $100 \times 100 \times 100$ grid of spacing 0.25Å) for the same representative solute structure.

Pairwise Energy Function Decomposition. Since it was of interest to see whether the complex interaction behavior observed in the MD simulations could be described by simpler energy functions, the 4D-FESs were used as references for extraction of pairwise "effective" energy functions. A number of methods for deriving simplified effective potentials from higher-dimensional systems have been reported previously;[62,68,69] the specific methodology used here will be described in detail in a future publication. Briefly, we used a standard Monte Carlo (MC) scheme to simultaneously optimize three separate 1D energy functions ($C_{carboxyl}-N_{amino}$, $C_{methyl}-C_{methyl}$, and $O_{carboxyl}-N_{amino}$) so that a 4D-FES computed using these (assumed additive) energy functions reproduced as well as possible the 4D-FES obtained from MD. A single $O_{carboxyl}-N_{amino}$ energy function was fitted because the two Oxygen–Nitrogen dimensions in the 4D-FES should—by symmetry—be identical, and the optimization procedure was conducted using only data from the MD simulations in which all four of the distances were between 2 and 15 Å. Initial "guesses" for each 1D energy function were made by randomly assigning free energy values at each distance (in 0.2 Å intervals) within the range ±0.5 kcal/mol; this ensured that no prior knowledge of the "true" 1D energy functional form was used in the optimization of the energy functions. Using these initial guessed energy functions, a trial 4D-FES was constructed and an initial average error of this FES relative to the actual MD 4D-FES was calculated. A Monte Carlo procedure was then conducted in which one of the three 1D energy functions was selected at random, and a random alteration (within the range ±1 kcal/mol) was made to the energy function at a distance chosen at random in the range from 2 to 15 Å. The new trial 1D energy function was used to recompute the 4D-FES and a Metropolis test[70] was used to determine whether to accept or reject the new energy function based on whether the average error obtained with the new energy function was lower than that obtained with the previous energy function. This MC optimization was conducted for a total of 30 000 steps with the only quirk being that for the first 5000 steps only the $O_{carboxyl}-N_{amino}$ energy function was optimized; this helped to ensure that the long-range electrostatic interaction of the two solutes was described only by this function and did not, for example, end up being partially described by the more intuitively short-range $C_{methyl}-C_{methyl}$ function. The entire optimization procedure was independently repeated 200 times and the 200 sets of three energy functions averaged to produce the final functions reported in Results; in practice, the 200 independent energy functions thus obtained were all very similar to one another, suggesting that together they represent a unique solution for fitting the 4D-FES. Finally, the quality of the fits was visually assessed: 2D-FESs were constructed by scoring 100 million random configurations of the solutes with the averaged pairwise 1D energy functions; these pairwise-computed 2D-FESs could then be compared directly with the corresponding MD 2D-FESs (see Results).

Results

Free Energy Surface for Acetate-Methylammonium Association in Water. A series of 500 ns MD simulations was used to compute the interaction free energy of acetate and methylammonium for all possible intersolute geometries in pure water and aqueous NaCl solutions. Interaction free energies were obtained by analysis of histograms of the intersolute atomic distances sampled during the simulations. Obviously, in terms of the degrees of freedom of the solutes a complete interaction free energy surface might be considered to have 8 dimensions, since there are 4 non-hydrogen atoms on acetate × 2 non-hydrogen atoms on methylammonium. Since sampling this 8 dimensional space would be challenging, and visualizing it even more so, a more convenient way of viewing the free energy surface is to limit it to 2 dimensions; we therefore focus most of our analysis on 2D free energy surfaces (2D-FESs), the natural choice of coordinates for which are the charge–charge distance and hydrophobic–hydrophobic distance (see Methods).

The 2D-FES obtained from the MD simulation performed in pure water is shown in Figure 2 along with schematic structures illustrating relevant minima on the surface. Despite the simplicity of the solutes, the 2D-FES is quite complex and contains a number of distinct free energy minima and maxima. As indicated schematically, structures along the upper edge of the diagonal are those where the primary associating factor is the charge–charge interaction; following this mode of association along the diagonal, three distinct minima are observed: a deep free energy minimum corresponding to a direct contact of the two charged

(67) Kastenholz, M. A.; Hünenberger, P. H. *J. Phys. Chem. B* **2004**, *108*, 774–788.
(68) Lyubartsev, A. P.; Laaksonen, A. *Phys. Rev. E* **1995**, *52*, 3730–3737.
(69) Apostolakis, J.; Hofmann, D. W. M.; Lengauer, T. *Acta Crystallogr. A* **2001**, *57*, 442–450.
(70) Metropolis, N.; Rosenbluth, A. W.; Rosenbluth, M. N.; Teller, A. H.; Teller, E. *J. Chem. Phys.* **1953**, *21*, 1087–1093.

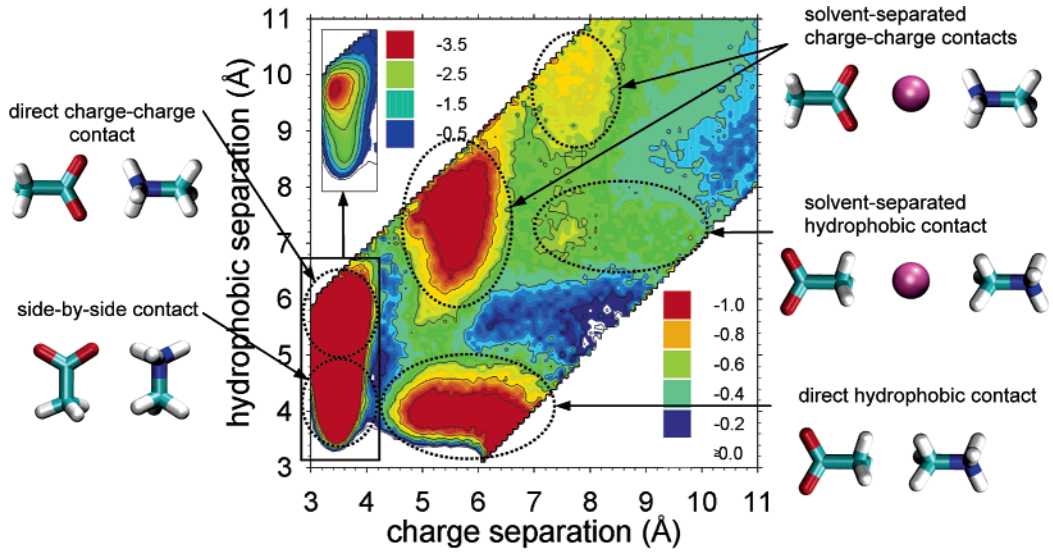

Figure 2. Two-dimensional free energy surface (2D-FES) for association of acetate and methylammonium computed from MD simulations in pure water (in kcal/mol). The inset at top left shows the charge−charge contact minima on an expanded energy scale in order to allow the position of the global minimum on the 2D-FES to be identified. Schematics indicating the approximate structures of energy minima of interest are shown (see text for details).

groups and two local minima corresponding to solvent-separated contacts. Structures along the lower edge of the diagonal are those where the primary associating factor is the hydrophobic (methyl−methyl) interaction; for this mode of association two clear free energy minima are observed, again corresponding to direct and solvent-separated configurations. It is apparent from the figure that in terms of relative strength the charge−charge interaction is much the greater; in fact, as shown in the inset, the interaction free energy of the actual direct contact minimum is ∼−3.5 kcal/mol for the charge−charge interaction, whereas that of the direct contact for the hydrophobic interaction is ∼−1.0 kcal/mol.

There are two other features of the pure water 2D-FES that are worth noting. First, the elliptical shape of the free energy minimum for the direct hydrophobic contact indicates that for the solute configurations that correspond to this minimum the methyl−methyl distances are considerably more constrained than are the charge−charge distances: the latter can apparently adopt a broad range of values (from ∼4.5 to ∼6.5Å). The probable explanation for this is that the hydrophobic contact is not directionally specific: there are therefore many possible, *isoenergetic* ways to arrange the two solutes such that their methyl groups are in direct contact. In effect then the charge−charge interaction distance is afforded a considerable amount of "wiggle room" in the solute configurations in which the methyl groups are in direct contact.

A second interesting feature is revealed by comparing free energy pathways for interconverting structures on the 2D-FES. If we consider as a starting point the side-by-side solute configuration (in which the two methyl groups are in direct contact with each other and the charged groups are also in direct contact with each other), then there are two simple pathways by which geometries representing other local minima can be reached. One pathway involves keeping the methyl−methyl distance fixed at 4.0 Å and rotating the charged groups away from each other until a collinear arrangement of the two solutes is attained (Figure 3). Perhaps not surprisingly, a significant free energy maximum is encountered along this pathway as increasing the distance between the two charged groups

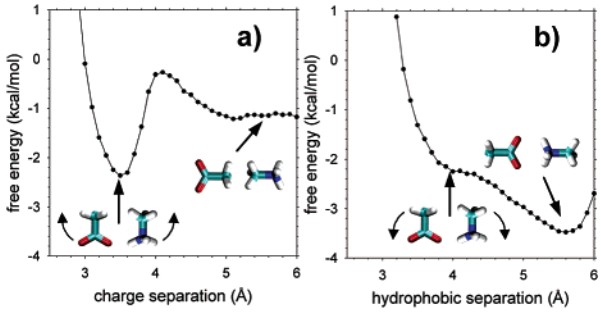

Figure 3. (a) Free energy profile obtained by rotating the charged groups of the acetate-methylammonium pair away from each other with the C_{methyl}−C_{methyl} distance held constant at 4.0 Å. (b) Free energy profile obtained by rotating the methyl groups of the acetate-methylammonium pair away from each other with the $C_{carboxyl}$−N_{amino} distance held constant at 3.4 Å. Both free energy profiles taken from the MD simulation in pure water.

diminishes their direct Coulombic interaction more rapidly than it is compensated by increased hydration. Once this free energy maximum is overcome, however, the broad local minimum geometry is reached in which relatively free motion of the charged groups is allowed (see above). A second pathway that can be followed involves keeping the charge−charge distance fixed at 3.4 Å and rotating the two methyl groups away from each other. One might expect to find—as was seen following the first pathway—that a significant free energy barrier would also be encountered along this pathway, especially so given that MD-computed potentials of mean force for methane-methane dissociation usually show a significant free energy maximum separating a direct contact from a solvent separated contact.[24] In fact, however, a maximum is not seen, and the interaction free energy smoothly decreases to the global minimum on the 2D-FES. The most likely explanation for this behavior is that the charge−charge interaction—in contrast to the methyl−methyl interaction—is directionally specific, and that it becomes much more favorable when the two charged groups face each other than when they lie alongside one another. The strong improvement in the charge−charge interaction caused by rotation of the methyl groups therefore likely masks the presence of any free energy maximum caused by separation of the methyl

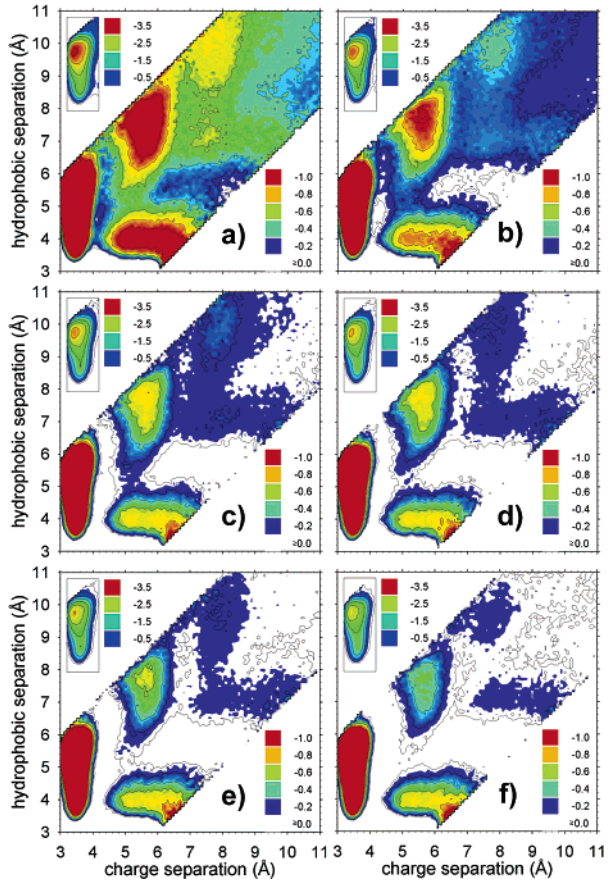

Figure 4. Two-dimensional free energy surfaces (2D-FESs) for association of acetate and methylammonium computed from MD simulations in salt solutions (in kcal/mol). Panels (a) through (f) show 2D-FESs obtained for NaCl solutions of concentration 0, 0.1, 0.3, 0.5, 1, and 2 M, respectively.

groups: this provides one demonstration therefore of the difficulties in dissecting out hydrophobic and charge−charge interactions from the observed behavior.

Effects of Salt on 2D Free Energy Surfaces for Acetate-Methylammonium Association. The 2D-FESs obtained for the five NaCl concentrations investigated (Figure 4) are all qualitatively similar to those of pure water (Figure 2) but the depths of free energy minima and the heights of energy maxima differ significantly. Importantly, these changes all occur smoothly, and there is a gradual, monotonic transition in the appearance of the 2D-FESs as the salt concentration increases from 0 M to 2 M NaCl: this provides one simple indication that the free energy surfaces obtained from the simulations are converged.

As the NaCl concentration increases, the depths of the three free energy minima that are primarily associated with the charge−charge interaction all become noticeably less favorable: this result is to be expected given the known salt dependence of salt bridge interactions.[71] Notably, however, the three minima all remain clearly visible even at the very high salt concentration 2 M, where it is often assumed that electrostatic interactions are completely screened. Addition of NaCl also slightly affects the two free energy minima that are primarily associated with hydrophobic interactions since they become somewhat less favorable as the NaCl concentration increases from 0 to 0.3 M; upon further addition of NaCl however the depths of these free energy minima remain essentially unchanged. This behavior contrasts with that seen in previous MD simulations examining the effects of salt on methane-methane interactions,[24] which have shown that such purely hydrophobic interactions are significantly stabilized by the addition of salt. It turns out however that the discrepancy is simply another manifestation of the difficulties in separating out the hydrophobic and charge−charge effects from the present simulations: in fact, as shown below, when a "true" hydrophobic interaction is extracted from the MD data, its salt dependence is in much closer agreement with expectations.

Comparison of MD Free Energy Surfaces with PB Free Energy Surfaces. The availability of converged association free energy surfaces obtained from explicit solvent-explicit salt MD simulations provides an excellent opportunity to test predictions made by the more computationally rapid but approximate PB theory. As noted in the Introduction, the use of PB in the present context introduces two major simplifications: (a) solvent is treated as a dielectric continuum, and (b) dissolved ions are modeled as continuous distributions obtained via a Boltzmann relationship to the electrostatic potential.[28] The consequences of the first simplification can be addressed simply by comparing the 2D-FES obtained from the MD simulations in pure water with a 2D-FES computed by solving the Poisson equation—since this is what the PB equation reduces to when the ionic strength is zero—for structural snapshots extracted from the MD simulations (see Methods). This comparison is shown in the upper panels of Figure 5. Not surprisingly, since the PB methodology treats the solvent as a continuum it does not adequately capture the presence of multiple maxima and minima on the surface: these features are reflections of the molecular nature of the solvent. However, despite these anticipated problems in capturing the local features of the 2D-FES, it is clear that the global appearance of the PB 2D-FES is actually in very good accord with that of the MD 2D-FES.

This encouraging impression is amplified considerably when the adequacy of the PB method's second assumption—a continuum description of the salt—is investigated. This is most easily done by subtracting the 2D-FES obtained in pure water from the 2D-FES computed at a salt concentration of interest for both MD and PB results: since this subtraction largely cancels out the errors due to the implicit-solvent approximation it allows the salt dependence predicted by the PB method to be compared directly with the salt dependence obtained from the MD simulations. When these comparisons are made, it is apparent that the PB calculations perform rather well. Figure 5c,d compares the MD and PB 2D-FESs obtained from the difference of the 0.1 M and 0 M surfaces; Figure 5e,f compares the results obtained from the difference of the 2 M and 0 M surfaces (a comparison of the absolute 2D-FESs is provided in Figure S3). In both MD and PB, the addition of salt destabilizes all solute−solute configurations; as might be expected, however, destabilization is greater for those configurations in which the charged groups of the solutes are close. Interestingly, the most obvious region of disagreement between MD and PB for the 0 M → 2 M salt dependence is where the (hydrophobic) methyl groups of the solutes are in direct contact (Figure 5e,f). In all probability, this arises because the PB calculations capture only the effects of salts on electrostatic interactions, and do not describe their effects on hydrophobic interactions; one way that the latter might be incorporated in future would be via inclusion

(71) Smith, J.; Scholtz, J. M. *Biochemistry* **1998**, *37*, 33−40.

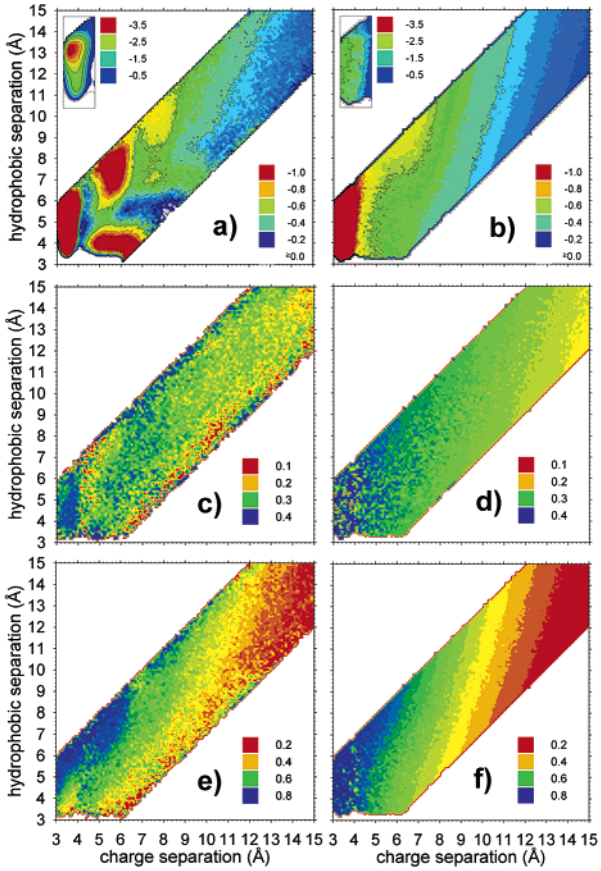

Figure 5. Comparison of two-dimensional free energy surfaces (2D-FESs) for association of acetate and methylammonium computed from MD simulations and PB calculations (in kcal/mol). Panels (a) and (b) show MD and PB results respectively for pure water. Panels (c) and (d) show the 0 M → 0.1 M salt dependence obtained from MD and PB, respectively. Panels (e) and (f) show the same for the 0 M → 2 M salt dependence. Note that while different energy scales are used for the different salt dependences to aid visualization, all MD−PB comparisons use identical energy scales.

of a solvent accessible surface area-based term as has been done recently.[34] That said, the generally good agreement in regions of the 2D-FES dominated by the charge−charge interaction provides important new support for the use of PB calculations for describing the effects of salt on molecular associations.

Comparison of Ion Distributions Obtained from MD and PB. A second test of the adequacy of PB's modeling of salt effects is to compare the ion distributions obtained from the theory with those extracted directly from the MD simulations; it should be recognized however that this is a stringent test, and it should not be expected that PB will perform perfectly for the same reason that we do not expect PB to correctly describe the maxima and minima on the pure water 2D-FES (see above). We focus on the distribution of ions around the direct contact and solvent-separated charge−charge free energy minima; comparisons for each of these configurations are shown in Figure 6 with the distributions obtained from MD (solid surfaces) and PB (wiremesh surfaces) being contoured at the same concentrations. One clear discrepancy that is present in all cases is that negative ions consistently approach much closer to the methylammonium in the PB calculations than they do in the MD simulations. This can be rectified by introducing an ion-exclusion radius into the calculations as is commonly done in PB calculations (see Methods) but this comes at the expense of a correspondingly poorer description of the distribution of

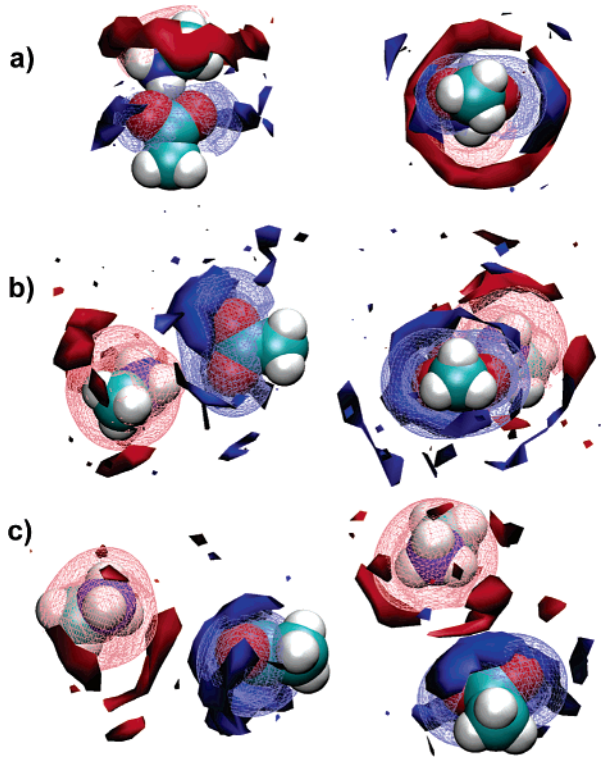

Figure 6. Comparison of ion distributions obtained from MD and PB around selected solute configurations; concentration isosurfaces obtained from MD are shown as solid, those obtained from PB are shown as wiremesh. For each of the three solute configurations investigated, two roughly perpendicular views are shown. (a) the direct charge−charge contact, (b) the first solvent-separated charge−charge contact, (c) the second solvent-separated charge−charge contact. In panels (a) and (b) surfaces are contoured at 0.9 M salt concentrations; in panel (c) surfaces are contoured at 1.2 M. Blue and red surfaces represent distributions of Na^+ (positive) ions and Cl^- (negative) ions, respectively.

positive ions and a generally worse agreement between the MD and PB 2D-FESs (Figure S4).

For the (global minimum) direct contact (Figure 6a), it is first important to note that the acetate and methylammonium are preferentially arranged in a "bent" configuration, not collinear as one might expect; this appears to be because in this configuration a polar amine hydrogen is neatly tucked between the two negatively charged carboxyl oxygens of the acetate (notably, the preference for a bent configuration is *not* simply a consequence of there being a larger number of bent configurations than linear configurations since this effect has been canceled out in the free energy surface calculations: see Methods). For this direct contact configuration, the ion distributions computed from PB are in reasonable agreement with the distributions obtained from the MD simulations. In MD, Na^+ ions localize in the plane of the acetate carboxylate group adjacent to the oxygens, whereas Cl^- ions form a more diffuse ring around the methylammonium. In the PB calculations, this behavior is reversed: the positive ion density tends to be more diffusely distributed around the acetate while the negative ion density is localized on the far side of the methylammonium as distant as possible from the acetate. Despite these differences, the overall local ion concentrations predicted by MD and PB are in quite close agreement.

The ion distributions for the first solvent-separated charge−charge interaction (Figure 6b) exhibit a more substantial disagreement between PB theory and the MD simulations. In

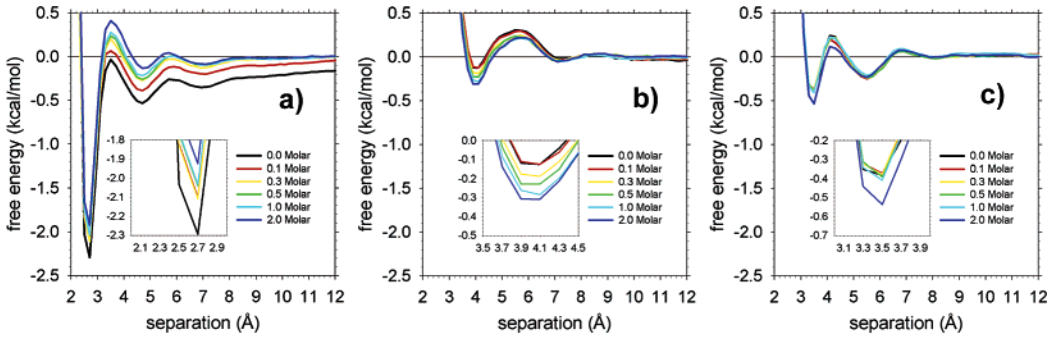

Figure 7. Pairwise effective energy functions obtained from independent Monte Carlo-based decompositions of the MD 4D-FESs obtained for each NaCl solution (see Methods for details). (a) the $O_{carboxyl}-N_{amino}$ energy function, (b) the $C_{methyl}-C_{methyl}$ energy function, (c) the $C_{carboxyl}-N_{amino}$ energy function. In each panel, the inset highlights the salt dependence of the global minimum of the energy function.

the MD simulations the ion distributions are similar to those seen in the direct contact minimum and there is no indication that either Na^+ or Cl^- ions localize directly between the two solutes: this suggests therefore that in MD this is exclusively a water mediated contact. In contrast, the PB calculations show significant concentrations of both negative and positive ions intervening between the two solutes. This is a qualitative discrepancy between the two methods attributable in the present case to the continuous—rather than discrete—description of the ions in PB theory; again however it is worth noting that this effect can be avoided by imposition of an ion exclusion radius (Figure S5). Interestingly, for the second solvent-separated charge−charge minimum—in which two solvent layers intervene between the solutes—better agreement is obtained between the PB predictions and the MD results (Figure 6c). Perhaps of most interest is the fact that in the MD simulations *both* Na^+ and Cl^- ions are seen to localize in the inter-solute region, indicating that the interaction between the two solutes at this point on the 2D-FES may be mediated at least some of the time by a Na^+/Cl^- ion pair. This behavior is nicely captured by the present PB calculations, but importantly is not reproduced by PB calculations that include an ion-exclusion radius (Figure S5).

Extraction of Pairwise Effective Energy Functions. Although the 2D-FESs obtained from MD provide the most natural way of visualizing the interaction free energy between the two solutes and explicitly recognize that there is an inter dependence of the charge−charge and hydrophobic interactions, this interdependence makes it difficult to unambiguously assess the relative contributions from the two types of interactions. In the present case, this is particularly problematic for the hydrophobic interaction, which appears to be swamped by the much stronger charge−charge interaction in at least two ways that have already been discussed: (a) the salt dependence of the interaction free energy for the direct hydrophobic contact does not correspond with that obtained by others for MD simulations of methane-methane interactions,[24] and (b), there is no apparent free energy maximum encountered when the methyl groups are separated from one another and the charged groups are held in direct contact (Figure 3b). In an attempt to circumvent this problem, and obtain a more direct view of the effects of salt on charge−charge and hydrophobic interactions, we have developed a simple Monte Carlo scheme aimed at finding optimized pairwise effective energy functions that best reproduce the FESs obtained from MD. As detailed in Methods, this optimization process has been carried out—independently for each salt concentration—using 4D-FESs in which the additional dimensions are the two Oxygen−Nitrogen distances: the remaining four distances are modeled simply as hard-sphere interactions. Crucially, the optimization process makes no assumptions about the functional form of any of the energy functions and allows them to be adjusted arbitrarily at 0.2Å intervals; the extent to which *interpretable* energy functions are obtained therefore provides one indication of the method's utility.

Figure 7a shows the energy functions obtained for the $O_{carboxyl}-N_{amino}$ distance for all salt concentrations studied. We anticipate that this function should provide the best representation of a pure charge−charge interaction, and it is therefore encouraging to find that the derived functions have a clear Debye−Hückel-like dependence on salt at long distances. Closer in, the energy function also has the expected solvent-separated and direct-contact minima, and as discussed below, the behavior of these peaks provides a surprisingly ready explanation for the salt dependence of protein−protein association and dissociation kinetics. Figure 7b shows the energy functions derived for the hydrophobic $C_{methyl}-C_{methyl}$ distance. Again, the functions have a readily interpretable shape—similar to the PMFs obtained by others for methane-methane interactions[24]—and with an expected decay to zero at long distance. Notably, a free energy maximum intervenes between the direct-contact and solvent-separated minima, which was masked by the charge−charge interaction in the rotational energy profile (Figure 3b). In addition, and most interestingly, the salt dependence of the direct-contact free energy minimum in the derived hydrophobic energy function is the same − both qualitatively and quantitatively—as that obtained in MD simulations of methane−methane interactions: [24] the direct-contact minimum is computed to be stabilized by 0.2 kcal/mol by increasing the NaCl concentration from 0 to 2 M, which corresponds exactly with that obtained by Garde and co-workers for methane-methane.[24] Moreover, the monotonic change of the free energy minimum with salt (Figure 7b; inset) provides a further argument in support of the precision of the MD results. The third derived energy function (Figure 7c)—that for the $C_{carboxyl}-N_{amino}$ distance—has behavior that is less easily interpreted; it should be noted however that this pair of atoms rarely come into direct contact with each other and that the interaction between the amino group and the carboxyl group is instead in effect always mediated by direct contacts between the N_{amino} and the $O_{carboxyl}$ atoms. Because of this, it might be too much to expect that this energy function's behavior would be physically interpretable; it is however encouraging to note that, with the exception of the 2 M case, it is salt-independent, which indicates that the salt dependence is instead primarily

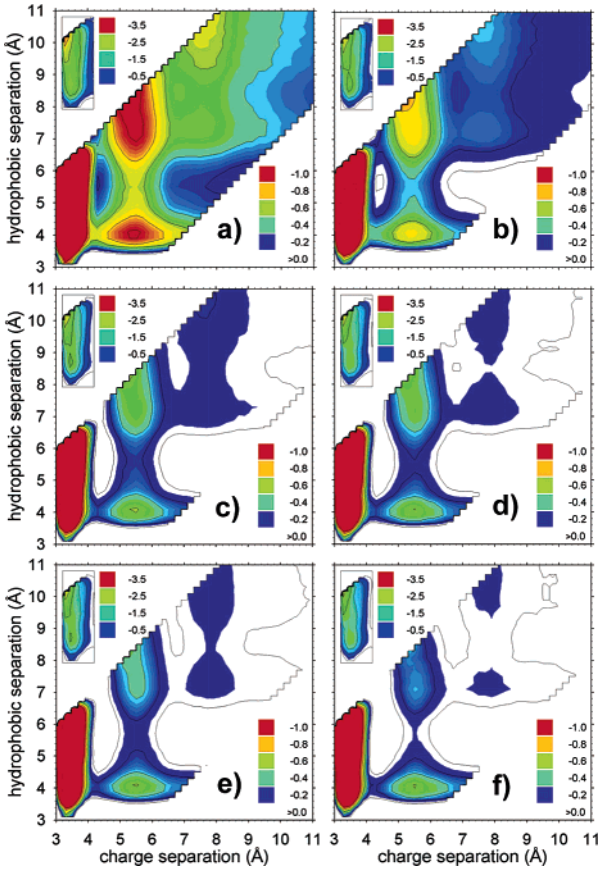

Figure 8. Two-dimensional free energy surfaces (2D-FESs) for association of acetate and methylammonium computed from Monte Carlo optimized 1D energy functions in salt solutions (in kcal/mol). Panels (a) through (f) show 2D-FESs obtained for NaCl solutions of concentration 0, 0.1, 0.3, 0.5, 1, and 2 M, respectively. These surfaces can be compared with those in Figure 4.

captured by the more easily interpreted hydrophobic and charge−charge functions. Despite this, it is probably more reasonable to view the $C_{carboxyl}-N_{amino}$ simply as an extra fitting parameter that aids the description of the orientational or angular dependence of the association. It is likely that alternative methods might be used to describe this orientational dependence, e.g., an explicit grid-based approach such as that which has been recently proposed for describing $\varphi-\psi$ dependences in amino acids.[72]

Figure 8 provides the "acid test" of the derived effective energy functions: their ability to reproduce the actual 2D-FESs obtained from MD simulations. The agreement is actually quite good, and although the magnitudes of the various free energy minima and maxima are not always quantitatively described, their positions on the 2D map are well reproduced. Since these structural features are not reproduced at all by PB calculations (Figure 5b) it appears that the energy functions derived here might eventually provide a viable—and extremely rapid to compute—alternative to PB calculations of intermolecular interaction free energies. It is of course likely that a closer correspondence between the 2D-FES approximated with pairwise energy functions and the actual MD 2D-FES could be achieved by optimizing the other four distances currently modeled as hard-sphere interactions, but this might come at the expense of more limited interpretability of the resulting functions.

Discussion

Since the work reported here describes the use of MD simulations, comparisons with PB theory, and a possible route to developing new pairwise energy functions, it contains a number of results that require further comment. One important result of the MD simulations, which is immediately apparent in the 2D-FESs shown in Figure 4, is that while the inter-solute charge−charge interaction is subject to significant screening by NaCl, a strong favorable interaction between the ammonium and carboxylate groups persists even at 2 M NaCl. This result is consistent with experimental tests of salt effects on charged side chains in designed α-helical peptides[71] and recent work suggesting that weak Hofmeister salts such as NaCl have a limited ability to screen electrostatic interactions.[73] It is however in contrast with the view often expressed in the literature that charge−charge interactions are completely screened at high salt,[38] and in fact, it is common for experimental behavior of an electrostatically driven system at high salt to be used as a proxy for how the same system might behave in the absence of any electrostatic interactions. If correct, then the present MD results would indicate that this view is suspect.

A finding that provides substantial support for the present MD results is that they successfully capture the very different salt dependences of the association and dissociation kinetics of charge−charge interactions. As has been discussed in detail by Zhou recently,[39] the experimental association rate constants for electrostatically driven protein−protein interactions depend linearly on the square root of the salt concentration whereas the experimental dissociation rate constants for the same systems are effectively independent of salt. Zhou[39] has considered these differences in terms of the differential stabilizing effects of salt on the protein−protein complex, the transition state for association and the unbound proteins using a Debye−Hückel model of electrostatic interactions. It is therefore interesting that these same observations can also be rationalized using results obtained from the present explicit salt-explicit solvent MD simulations. Figure 9a plots the salt dependence of the free energy barrier to association obtained from the $O_{carboxyl}-N_{amino}$ 1D energy function shown in Figure 7a; interestingly, this observed salt dependence fits with an r^2 value of 0.97 to the theoretical expression derived by Zhou.[39] Figure 9b plots the salt dependence of the free energy barrier to dissociation of the direct-contact minimum obtained from the $O_{carboxyl}-N_{amino}$ 1D energy function; in line with experimental results for dissociation of electrostatically driven protein−protein complexes, it shows a much lower dependence on the NaCl concentration: the gradients of the lines shown in Figures 9a and 9b differ by approximately 4-fold. Although these results were obtained from the derived $O_{carboxyl}-N_{amino}$ pairwise energy function, essentially identical results are also obtained from 1D PMFs computed directly from MD histograms of the charge−charge distance (Figure S6).

Because the MD simulations yield a view of salt effects that is both structurally detailed and thermodynamically refined, they

(72) Mackerell, A. D.; Feig, M.; Brooks, C. L. *J. Comput. Chem.* **2004**, *25*, 1400−1415.

(73) Perez-Jimenez, R.; Godoy-Ruiz, R.; Ibarra-Molero, B.; Sanchez-Ruiz, J. M. *Biophys. J.* **2004**, *86*, 2414−2429.

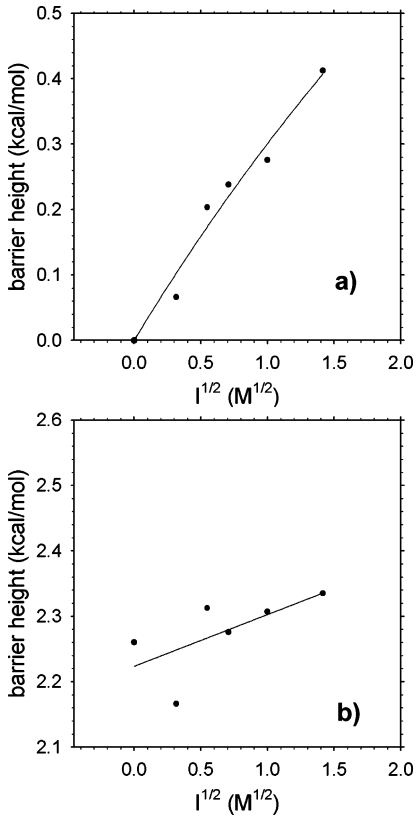

Figure 9. Salt dependence of barrier heights taken from the $O_{carboxyl}-N_{amino}$ 1D energy function shown in Figure 7a. (a) the energy barrier for association, and (b) the energy barrier for dissociation of the direct charge−charge contact. Lines show the fits of the functional form proposed by Zhou (eq 20 in ref 39); r^2 values are 0.97 and 0.43 for panels (a) and (b), respectively.

also provide a valuable new benchmark for testing simpler implicit solvent models that might be used to simulate much larger systems, where obtaining converged thermodynamic results from explicit solvent simulations may be difficult. With this idea in mind, we have conducted an extensive comparison of the MD results with the predictions of PB theory: to our knowledge this is the first attempt to directly compare PB with explicit salt-explicit solvent MD results for an intermolecular association reaction. Overall, it appears that PB provides a rather good thermodynamic description of the effects of NaCl on the particular system studied here (Figure 5), thereby reinforcing its use for describing the effects of salt on binding thermodynamics.[4,31−34] As expected, however, PB cannot begin to describe all of the structural features of the MD-computed FESs, and in terms of developing a rapid energetic treatment for use in dynamic simulations it might be that a better approach is to derive specific pairwise energy functions by an optimization procedure such as the one outlined here. As shown by Figure 8 such energy functions can produce FESs that are in much closer agreement with MD results than those that might be obtained using PB theory. We are currently investigating therefore whether pairwise energy functions derived in this way might be transferable to different molecular systems.

Finally, any simulation study must consider potential deficiencies of the methods used, and one obvious concern in this regard is the validity of the force field parameters. The OPLS-AA force field used here is likely to perform equally well with respect to other fixed charge molecular mechanics force fields (see ref 74 and references therein), and importantly for the present application, the parameters for NaCl have been shown to produce structural properties in good agreement with experiment and with other NaCl parameter sets.[75] Although it is likely that quantitative differences in the FESs would be obtained with alternative parameter sets, it is unlikely that qualitative differences (e.g., in the order of stabilities of minima) would result. This is particularly true for the salt dependent effects since gross errors in parameters will be canceled out by subtraction of FESs obtained in different salt concentrations.

Although the strength of the direct charge−charge contact interaction obtained here is similar to that seen in other MD studies of amino acid salt bridges in water,[76−79] it is to be noted that experimental estimates of the contributions of salt bridge interactions to protein stability are more generally in the range 0.5−1.5 kcal/mol.[71,80−82] This difference would seem to warrant further investigation: obvious factors that might contribute to the discrepancy are entropic penalties due to side chain restrictions (which will be present in real proteins but which are canceled out in our FESs) and local environmental influences that may modulate the interaction.[76,81] Although there perhaps is still some way to go before a direct connection between explicit solvent-explicit salt MD simulations and experimental studies of protein stability can be established, it would appear that simulations of the type reported here have the potential to provide fundamental insights into the effects of simple salts on molecular associations.

Acknowledgment. We are grateful to Andrej Sali for the suggestion of SD simulations as a reference state for free energy calculations. This work was supported in part by a grant from the Roy J. Carver Charitable Trust and a CAREER award (no. 0448029) from the National Science Foundation.

Supporting Information Available: Partial charges assigned to the acetate and methylammonium solutes; linear regression of MD and PB-computed interaction energies; illustration of "crystal" lattice used for computation of long-range periodic electrostatic interactions; comparison of absolute MD and PB 2D-FESs; comparison of MD and PB 2D-FESs computed with an ion-exclusion radius of 2 Å; comparison of MD and PB ion distributions around selected solute configurations computed with an ion-exclusion radius of 2 Å; salt dependences of association and dissociation energy barriers obtained from directly computed 1D PMFs of the charge−charge interaction. This material is available free of charge via the Internet at http://pubs.acs.org.

JA058637B

(74) Mackerell, A. D. *J. Comput. Chem.* **2004**, *25*, 1584−1604.
(75) Patra, M.; Karttunen, M. *J. Comput. Chem.* **2004**, *25*, 678−689.
(76) Kumar, S.; Nussinov, R. *Biophys. J.* **2002**, *83*, 1595−1612.
(77) Maksimiak, K.; Rodziewicz-Motowidlo, S.; Czaplewski, C.; Liwo, A.; Scheraga, H. A. *J. Phys. Chem. B* **2003**, *107*, 13496−13504.
(78) Masunov, A.; Lazaridis, T. *J. Am. Chem. Soc.* **2003**, *125*, 1722−1730.
(79) Hassan, S. A. *J. Phys. Chem. B* **2004**, *108*, 19501−19509.
(80) Makhatadze, G. I.; Loladze, V. V.; Ermolenko, D. N.; Chen, XF.; Thomas, S. T. *J. Mol. Biol.* **2003**, *327*, 1135−1148.
(81) Luisi, D. L.; Snow, C. D.; Lin, J.-J.; Hendsch, Z. S.; Tidor, B.; Raleigh, D. P. *Biochemistry* **2003**, *42*, 7050−7060.
(82) Iqbalsyah, T. M.; Doig, A. J. *Biochemistry* **2005**, *44*, 10449−10456.